frontiers | Frontiers in Earth Science

TYPE Original Research
PUBLISHED 11 January 2023
DOI 10.3389/feart.2022.901573

OPEN ACCESS

EDITED BY
Peter David Roopnarine,
California Academy of Sciences,
United States

REVIEWED BY
Olev Vinn,
University of Tartu, Estonia
Tian Jiang,
China University of Geosciences, China

*CORRESPONDENCE
Chen-Yang Cai,
cycai@nigpas.ac.cn

SPECIALTY SECTION
This article was submitted to Paleontology, a section of the journal Frontiers in Earth Science

RECEIVED 22 March 2022
ACCEPTED 31 October 2022
PUBLISHED 11 January 2023

CITATION
Li Y-D, Ślipiński A, Huang D-Y and Cai C-Y (2023), New fossils of Sphaeriusidae from mid-Cretaceous Burmese amber revealed by confocal microscopy (Coleoptera: Myxophaga). *Front. Earth Sci.* 10:901573. doi: 10.3389/feart.2022.901573

New fossils of Sphaeriusidae from mid-Cretaceous Burmese amber revealed by confocal microscopy (Coleoptera: Myxophaga)

Yan-Da Li[1,2], Adam Ślipiński[3], Di-Ying Huang[1] and Chen-Yang Cai[1,2]*

[1]State Key Laboratory of Palaeobiology and Stratigraphy, Nanjing Institute of Geology and Palaeontology, Chinese Academy of Sciences, Nanjing, China, [2]Bristol Palaeobiology Group, School of Earth Sciences, University of Bristol, Bristol, United Kingdom, [3]Australian National Insect Collection, CSIRO, Canberra, ACT, Australia

Sphaeriusidae is a small family of tiny aquatic beetles in the suborder Myxophaga. In this study we characterize two new sphaeriusid fossils from the mid-Cretaceous Burmese amber with the help of confocal laser scanning microscopy. *Sphaerius martini* Li & Cai **sp. nov.** displays similarities with both extant *Bezesporum* and *Sphaerius*, although it can be readily recognized based on the parallel-sided prosternum. *Crowsonaerius minutus* Li & Cai **gen. et sp. nov.** differs from other genera of Sphaeriusidae in having unreduced apical maxillary palpomeres, lowered mesoventrite, large metacoxal plates, separated mesotrochanter and mesofemur, and equal pretarsal claws. The present study demonstrates the efficacy of confocal microscopy in studying minute and dark bioinclusions in amber.

urn:lsid:zoobank.org:pub:6E6EDC20-744A-4A75-849A-4B6126628C15.

KEYWORDS

Sphaeriusidae, fossil, Burmese amber, confocal microscopy, Cretaceous

1 Introduction

The suborder Myxophaga is a comparatively small group of Coleoptera, with approximately 65 extant species (Mesaroš, 2013). Recent molecular phylogenies generally supported a sister-group relationship between Myxophaga and Archostemata (e.g., Mckenna et al., 2019; Cai et al., 2022). Although the earliest fossils of Myxophaga date back to the Late Triassic (Fikáček et al., 2020; Qvarnström et al., 2021), myxophagan fossils have only been very sparsely reported. Myxophaga currently comprises four extant families of minute aquatic or riparian beetles, i.e., Lepiceridae, Torridincolidae, Hydroscaphidae and Sphaeriusidae. However, the interrelationships among the four families remain unsettled, as morphology and molecular-based phylogenies have yielded inconsistent topologies (Beutel, 1999;

Lawrence et al., 2011; Mckenna et al., 2015, 2019; Yavorskaya et al., 2018; Jałoszyński et al., 2020).

Sphaeriusidae is a small but widespread family, with only two genera and about 25 species known in extant fauna (Lawrence & Ślipiński, 2013; Hall, 2019; Fikáček et al., 2022). The adults of Sphaeriusidae are easily characterized by the tiny and dorsally convex body, 11-segmented antennae, fused mesotrochanterofemora, large metacoxal plates, 3 (rarely 2)-segmented tarsi, and abdomen with only three ventrites of which the second is short (Reichardt, 1973; Löbl, 1995; Fikáček et al., 2022). As pointed out by Beutel & Raffaini (2003), due to the small size of sphaeriusids, detailed morphology for extant species can only be properly documented when SEM (scanning electronic microscopy) techniques are applied. However, only a few sphaeriusids have been imaged under SEM (e.g., Löbl, 1995; Liang & Jia, 2018; Yavorskaya et al., 2018; Fikáček et al., 2022), and some of them were not identified to species level (e.g., Beutel, 1999; Beutel & Raffaini, 2003; Kamezawa & Matsubara, 2012). As a result, the taxonomy of this group has been insufficiently studied and the its species-level diversity is likely strongly underestimated (Fikáček et al., 2022).

Due to their minute body size, sphaeriusids are rarely documented and often overlooked in the fossil record. The only two fossils known to date are *Burmasporum rossi* Kirejtshuk and *Bezesporum burmiticum* Fikáček et al., both from mid-Cretaceous Burmese amber (Kirejtshuk, 2009; Fikáček et al., 2022). However, some important characters were not observed for these two fossils, partly due to the usage of traditional brightfield imaging technique only. In this study we report two new species of Sphaeriusidae from the Burmese amber, and provide detailed photos obtained with confocal microscopy.

2 Materials and methods

2.1 Materials

The Burmese amber specimens studied herein originated from amber mines near Noije Bum (26°20′ N, 96°36’ E), Hukawng Valley, Kachin State, northern Myanmar. The amber specimens are deposited in the Nanjing Institute of Geology and Palaeontology (NIGP), Chinese Academy of Sciences, Nanjing, China. The amber pieces were trimmed with a small table saw, ground with emery paper of different grit sizes, and finally polished with polishing powder. The specimens of extant *Sphaerius* sp. for comparison were collected in Cabbage Tree Creek in New South Wales, Australia.

2.2 Imaging

Photographs under incident light were taken with a Zeiss Discovery V20 stereo microscope. Confocal images were obtained with a Zeiss LSM710 confocal laser scanning microscope, mainly using the 488 nm Argon laser excitation line. Additional excitation wavelengths were also tested for comparison. The extant *Sphaerius* specimens were sputter-coated with gold and photographed with a Hitachi SU 3500 scanning electron microscope. Images were stacked in Helicon Focus 7.0.2 and Adobe Photoshop CC. Images were further processed in Adobe Photoshop CC to adjust brightness and contrast.

2.3 Phylogenetic analyses

To evaluate the systematic placement of the two new fossils, a constrained morphology-based phylogenetic analyses was performed under Bayesian inference. The data matrix (Supplementary Data S1, S2) was mainly derived from a recently published dataset (Fikáček et al., 2022). The definitions of some characters were modified to fit the inclusion of the new fossils and additional outgroups. The constraining backbone tree was constructed based on the molecular results by Mckenna et al. (2019) and Fikáček et al. (2022). Only the fossil taxa were allowed to move freely across the backbone tree (e.g., Fikáček et al., 2020; Li et al., 2022).

The Bayesian analysis was performed using MrBayes 3.2.6 (Ronquist et al., 2012). Two MCMC analyses were run simultaneously, each with one cold chain and three heated chains. Trees were sampled every 1,000 generations. Analyses were stopped when the average standard deviation of split frequencies remained below 0.01. The first 25% of sampled trees were discarded as burn-in, and the remains were used to build a majority-rule consensus tree.

The tree was drawn with the online tool iTOL Version 6.6 (Letunic and Bork, 2021) and graphically edited with Adobe Illustrator CC 2017.

3 Systematic paleontology

Order Coleoptera Linnaeus, 1758.
Suborder Myxophaga Crowson, 1955.
Family Sphaeriusidae Erichson, 1845.

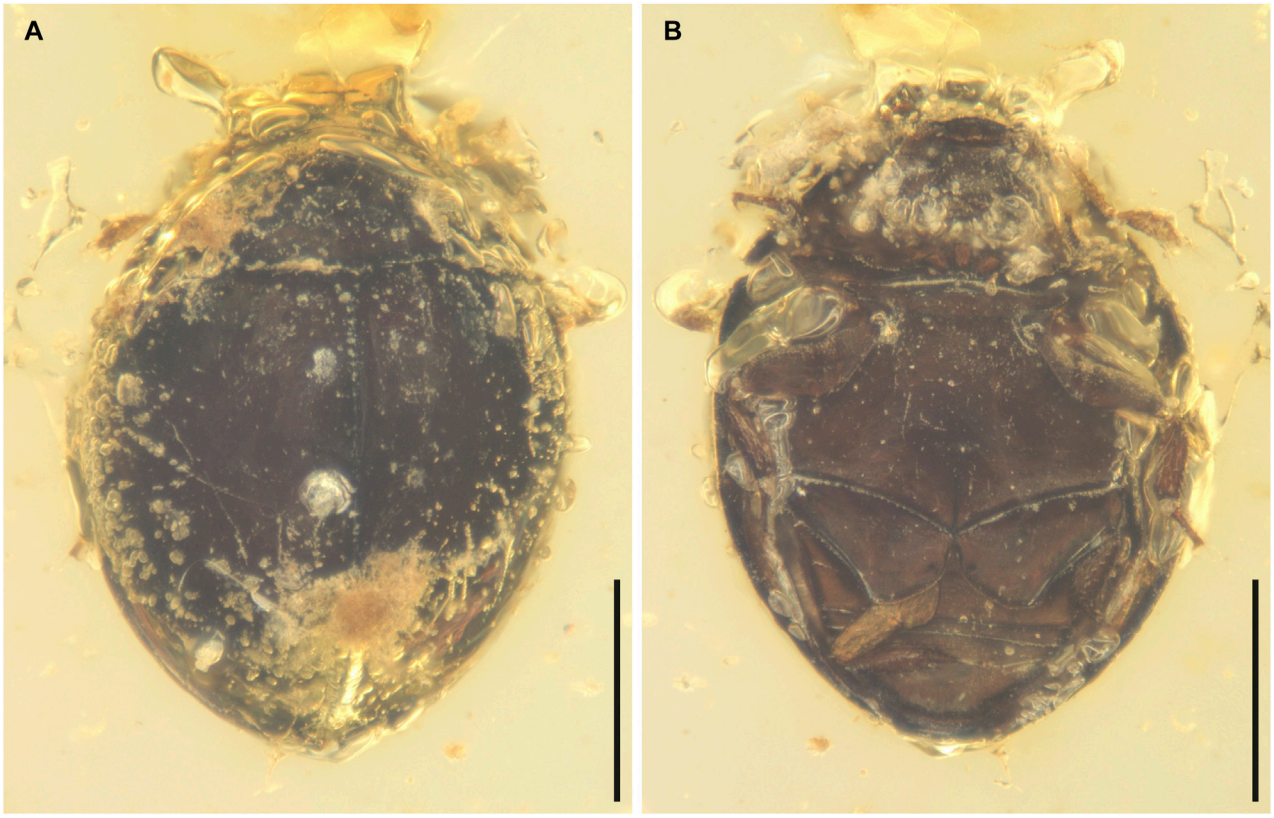

FIGURE 1
General habitus of *Sphaerius martini* Li and Cai sp. nov., holotype, NIGP178177, under incident light. **(A)** Dorsal view. **(B)** Ventral view. Scale bars: 200 μm.

3.1 *Sphaerius martini* Li & Cai sp. nov

3.1.1 Material

Holotype, NIGP178177 (Figures 1, 2), mid-Cretaceous (upper Albian to lower Cenomanian; Shi et al., 2012; Mao et al., 2018), from amber mine near Noije Bum Village, Tanai Township, Myitkyina District, Kachin State, Myanmar.

3.1.2 Etymology

The species is named after Dr. Martin Fikáček, an expert on aquatic beetles, who provided invaluable comments on the morphology of this fossil.

3.1.3 Diagnosis

Antennal club 4-segmented (Figure 2C). Prosternum parallel-sided (Figure 2C). Anterior margin of mesotrochanterofemur weakly sinuate (Figure 2B). Outer posterior edge of metacoxal plate slightly concave (Figure 2D). Metatarsus with very long setae (Figure 2D).

3.1.4 Description

Body broadly oval, strongly convex, about 0.60 mm long, 0.44 mm wide.

Head prognathous, short and broad. Antennal insertions exposed. Antennae 11-segmented with 4-segmented club; antennomeres 1 and 2 robust; antennomere 3 moderately elongated (about twice as long as 4); antennomeres 4–7 submoniliform; antennomeres 8–11 clubbed; antennomeres 9–11 with distinct setae. Mandibles flattened. Maxillary palps probably 4-segmented; apical palpomere distinctly shortened. Mentum subtrapezoidal, narrowing anteriad.

Pronotal disc convex, widest at hind angles. Scutellar shield small, triangular, posteriorly acute. Elytra complete, covering all abdominal segments. Prosternum parallel-sided. Mesoventrite relatively short, on the same plane with metaventrite, fused with the latter. Mesocoxae widely separated. Metaventrite broad, transverse. Metacoxae contiguous, extending laterally to elytra; metacoxal plates posteriorly not reaching abdominal ventrite 3, gradually narrowed laterally in outer half; outer posterior edge of metacoxal plate slightly concave. Legs short. Mesotrochanter fused with femur; anterior margin of mesotrochanterofemur

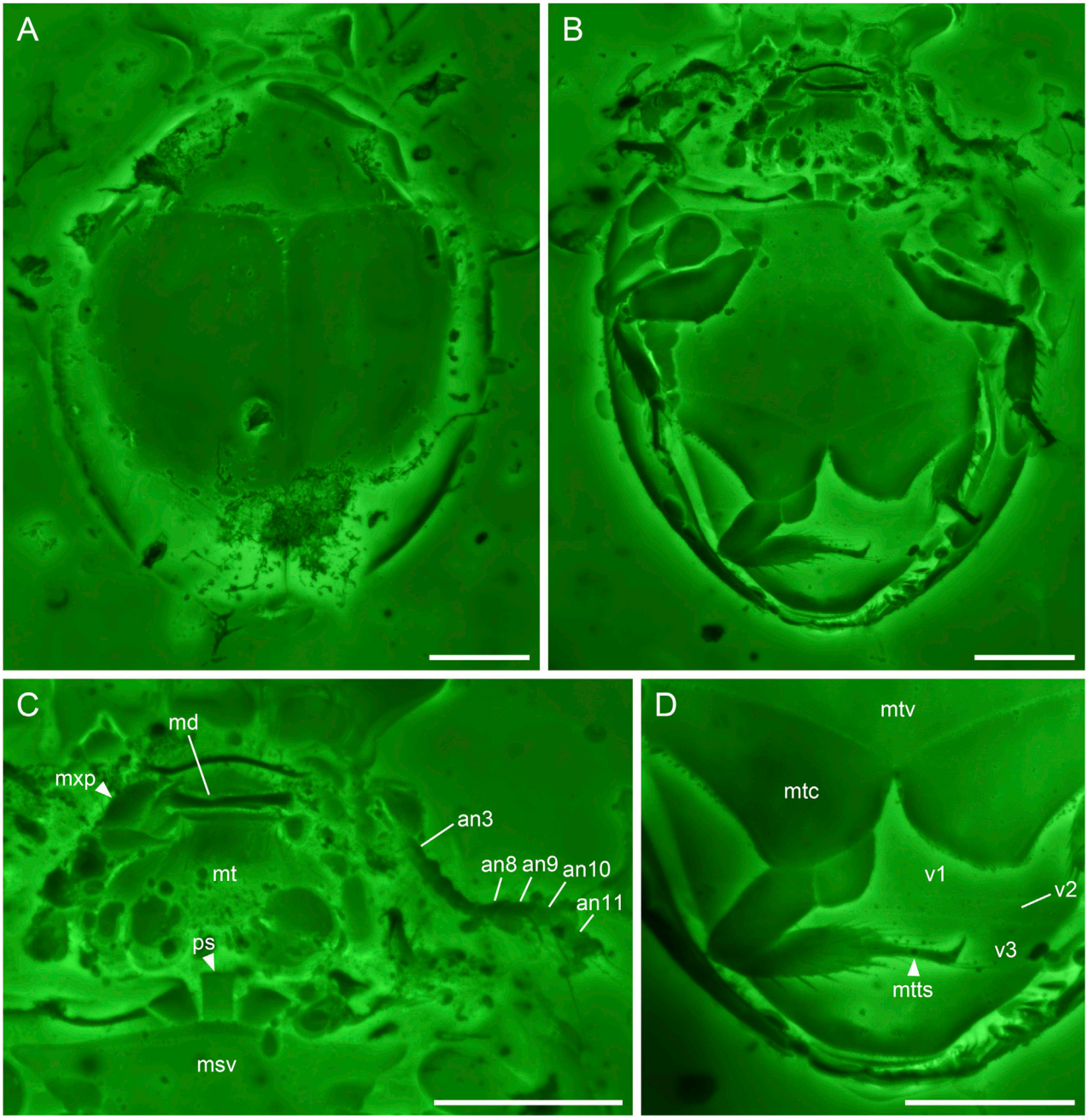

FIGURE 2
Sphaerius martini Li & Cai sp. nov., holotype, NIGP178177, under confocal microscopy. **(A)** Habitus, dorsal view. **(B)** Habitus, ventral view. **(C)** Head and prothorax, ventral view. **(D)** Hind leg and abdomen, ventral view. Abbreviations: an3–11, antennomeres 3–11; md, mandible; msv, mesoventrite; mt, mentum; mtc, metacoxa; mtts, metatarsus; mtv, metaventrite; mxp, maxillary palp; ps, prosternum; v1–3, ventrites 1–3. Scale bars: 100 μm.

weakly sinuate. Femora subglabrous. Tibiae and tarsi setose; metatarsus with very long setae. Pretarsal claws simple, unequal.

Abdomen with three ventrites; ventrite 2 distinctly shorter than ventrite 1 or 3.

3.1.5 Remarks

Sphaerius martini shares an overall similar morphology with extant Sphaeriusidae. It could be ruled out from the fossil genus *Burmasporum* Kirejtshuk based on the normal pronotal shape

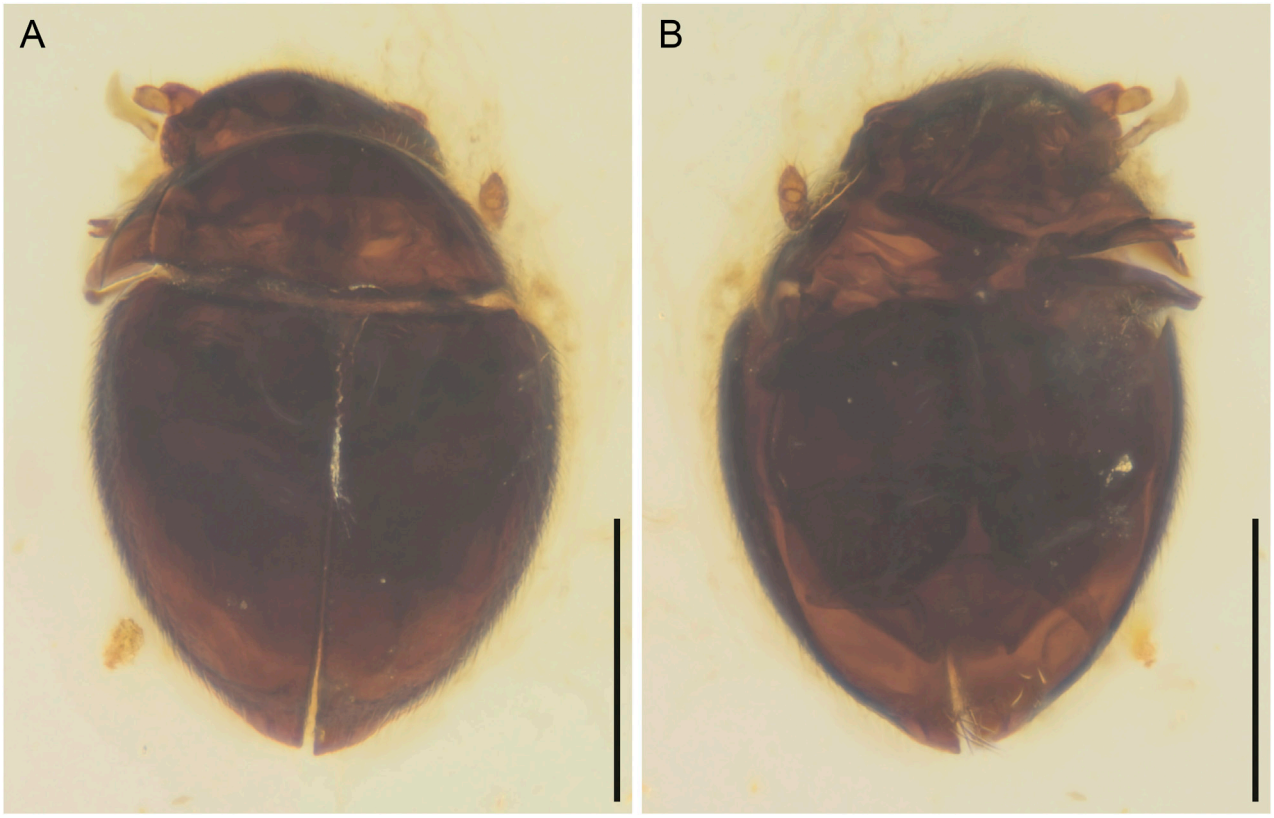

FIGURE 3
General habitus of *Crowsonaerius minutus* Li & Cai gen. et sp. nov., holotype, NIGP178178, under incident light. **(A)** Dorsal view. **(B)** Ventral view. Scale bars: 200 μm.

(Fikáček et al., 2022). Concerning the remaining two genera, the new species is tentatively assigned to *Sphaerius* Waltl, based on its subtrapezoidal mentum (Figure 2C), relatively short mesoventral plate (Figure 1B), and parallel-sided prosternum (Figure 2C) (mentum parallel-sided, mesoventral plate longer, and prosternum strongly T-shaped in *Bezesporum* Fikáček et al., 2022). Extant *Bezesporum* and aberrant *Sphaerius* (from Australia and South Africa) have strongly T-shaped (anteriorly expanded) prosternum. In other typical *Sphaerius* the prosternum is less T-shaped. The prosternum of *S. martini* is even narrower and parallel-sided, which is distinctive in Sphaeriusidae. *Sphaerius martini* differs from extant *Sphaerius* in having very long setae on metatarsus, and additionally from most *Sphaerius* species in having 4-segmented antennal club (see also Discussion). Some important characters were not possible to observe in the previously reported *Be. burmiticum*, which was also described from Burmese amber. Nevertheless, aside from the length of mesoventral plate, *S. martini* could also be differentiated from *Be. burmiticum* based on the shape of metacoxal plate. The outer posterior edge of metacoxal plate is slightly concave in *S. martini*, while that of *Be. burmiticum* is somewhat sinuate.

3.2 *Crowsonaerius minutus* Li & Cai gen. et sp. nov

3.2.1 Material

Holotype, NIGP178178 (Figures 3, 4), mid-Cretaceous (upper Albian to lower Cenomanian; Shi et al., 2012; Mao et al., 2018), from amber mine near Noije Bum Village, Tanai Township, Myitkyina District, Kachin State, Myanmar.

3.2.2 Etymology

The generic name (masculine in gender) is constructed based on the last name of Prof. Roy A. Crowson, in recognition of his great contribution to the systematics of Myxophaga, and the generic name *Sphaerius*, the type genus of Sphaeriusidae. The specific name refers to the minute size of the species.

3.2.3 Diagnosis

Antennae 11-segmented with 3(?)-segmented club (Figure 4C). Apical maxillary palpomere unreduced (compared to extant *Sphaerius*) (Figure 4C). Mesoventrite probably lower than metaventrite (Figure 4D). Metacoxal

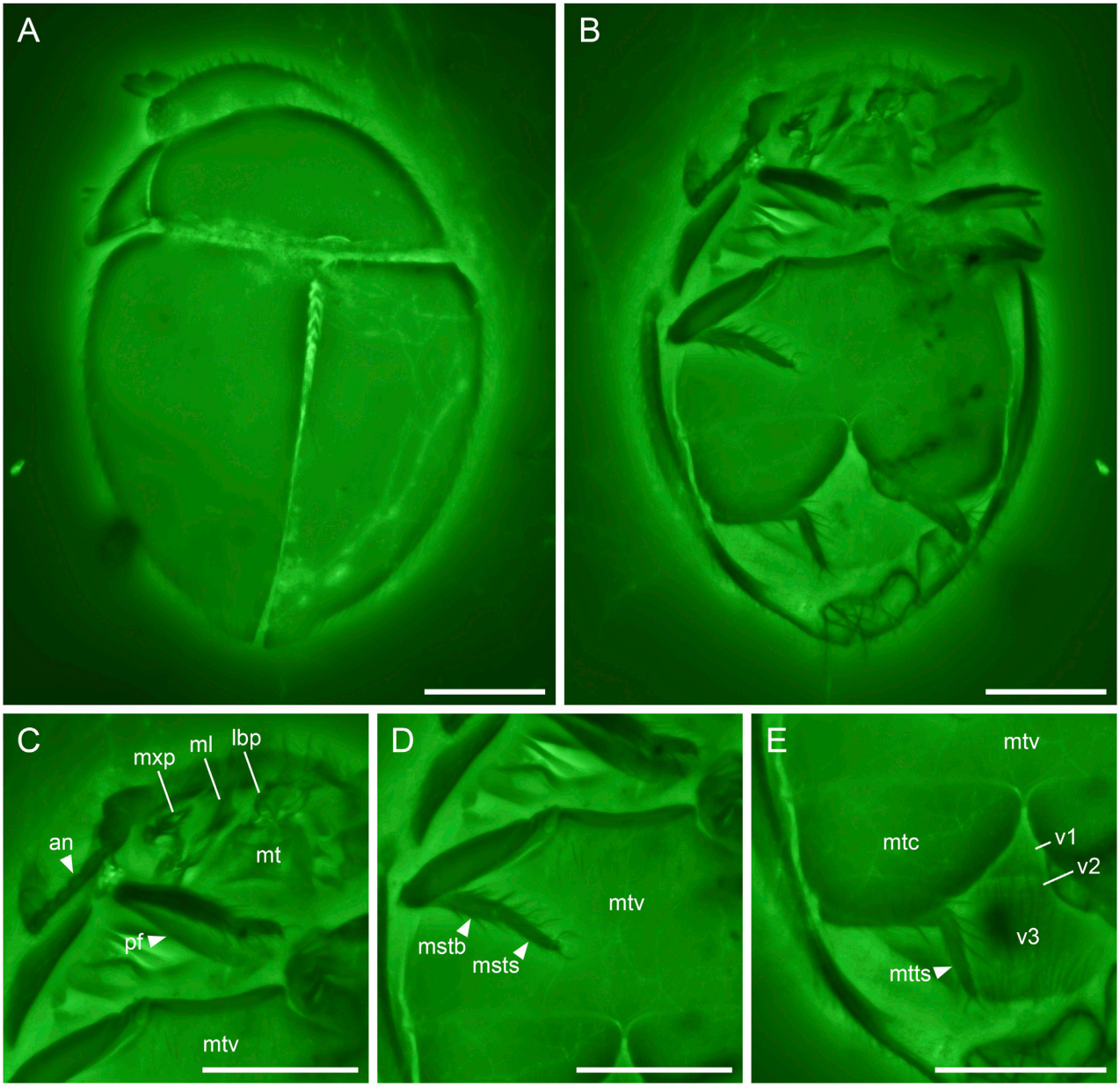

FIGURE 4
Crowsonaerius minutus Li & Cai gen. et sp. nov., holotype, NIGP178178, under confocal microscopy. **(A)** Habitus, dorsal view. **(B)** Habitus, ventral view. **(C)** Head and prothorax, ventral view. **(D)** Metathorax, ventral view. **(E)** Hind leg and abdomen, ventral view. Abbreviations: an, antenna; lbp, labial palp; mstb, mesotibia; msts, mesotarsus; ml, mala; mt, mentum; mtc, metacoxa; mtts, metatarsus; mtv, metaventrite; mxp, maxillary palp; pf, profemur; v1–3, ventrites 1–3. Scale bars: 100 μm.

plates nearly contiguous, not narrowed laterally (Figure 4E). Mesotrochanter not fused with femur (Figure 4D). Tarsi *Sphaerius*-like; metatarsus without very long setae. Pretarsal claws equal (Figures 4C–E). Abdomen with three ventrites of which the second is short (Figure 4E).

3.2.4 Description

Body broadly oval, strongly convex, about 0.49 mm long, 0.33 mm wide.

Head prognathous, short and broad. Antennal insertions exposed. Antennae 11-segmented with 3(?)-segmented club;

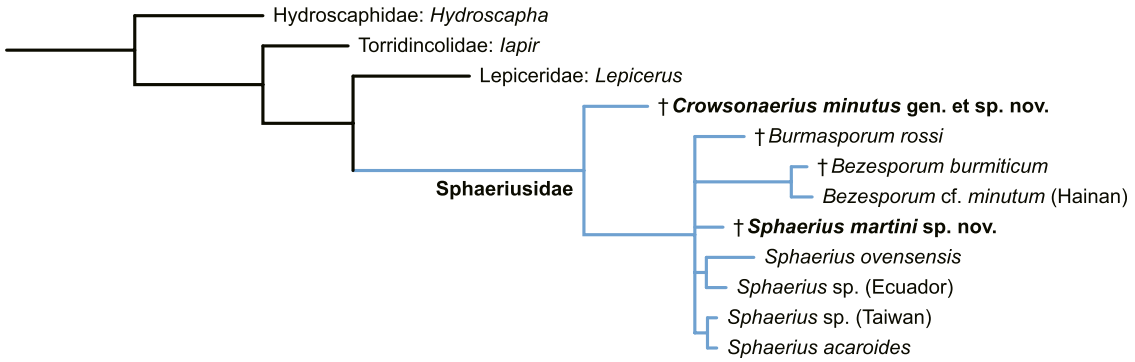

FIGURE 5
Suggested placement of *Sphaerius martini* and *Crowsonaerius minutus* within Sphaeriusidae. Tree resulting from the Bayesian analysis constrained by a molecular backbone tree.

antennomeres 1 and 2 robust; antennomere 3 moderately elongated (about twice as long as 4); antennomeres 9(?)–11 clubbed. Maxilla with undivided mala; maxillary palps 4-segmented; apical palpomere not distinctly shortened, seemingly apically pointed. Mentum subtrapezoidal, narrowing anteriad.

Pronotal disc convex, widest at hind angles. Scutellar shield small, triangular, posteriorly acute. Elytra complete, covering all abdominal segments. Mesoventrite not seen, probably lower than metaventrite. Mesocoxae widely separated. Metaventrite broad, transverse. Metacoxae nearly contiguous, extending laterally to elytra; metacoxal plates large, posteriorly reaching abdominal ventrite 3, gradually narrowed medially in medial half. Hind wing present; margin lined with setae. Legs short. Mesotrochanter not fused with femur. Femora glabrous. Tibiae and tarsi setose; metatarsus without very long setae. Pretarsal claws simple, equal.

Abdomen with three ventrites; ventrite 2 distinctly shorter than ventrite 1 or 3.

3.2.5 Remarks

The key character assigning *Crowsonaerius* to Sphaeriusidae is the abdomen with three ventrites of which the second is short (Figure 4E). Such an abdomen with three ventrites is unknown in any other beetle families (Lawrence et al., 2011). Additional characters excluding *Crowsonaerius* from other families in Myxophaga include the presence of antennal club (Figure 3B), elongated antennomere 3 (Figure 4C), and large and contiguous metacoxal plates (Figure 4E).

Crowsonaerius could be separated from all other sphaeriusid genera based on its equal pretarsal claws. In both *Sphaerius* and *Bezesporum*, as well as *Burmasporum*, one of the tarsal claws is strongly reduced in all three pairs of legs (Fikáček et al., 2022). *Crowsonaerius* also differs from other genera in the shape of metacoxal plate. *Sphaerius*, *Bezesporum* and *Burmasporum* have metacoxal plates gradually narrowed laterally, while in *Crowsonaerius* the edges of metacoxal plates are not laterally converged. The metacoxal plates of *Crowsonaerius* are also larger, reaching the posterior edge of ventrite 1. In addition, *Crowsonaerius* is distinctive in having a lowered mesoventrite (without clear mesoventral plate), and separated mesotrochanter and mesofemur. In extant *Sphaerius* and *Bezesporum*, the mesoventral plate is on the same plane with metaventrite and fused with the latter, and the mesotrochanter and mesofemur are fused together (Fikáček et al., 2022) (the states of these characters are unclear in *Burmasporum*). The apical maxillary palpomere of *Crowsonaerius* seems not to be distinctly reduced. Within Myxophaga, such a normal apical maxillary palpomere was previously only known in Lepiceridae, while in the other three families the apical maxillary palpomere is distinctly reduced.

The retention of equal pretarsal claws and separated mesotrochanter and mesofemur supports *Crowsonaerius* as the basalmost member within Sphaeriusidae (Figure 5).

4 Discussion

4.1 Morphological distinction between *Sphaerius* and *Bezesporum*

Extant sphaeriusids are generally highly uniform in external morphology, and has long been classified in a single genus. Only very recently, Fikáček et al. (2022) divided *Sphaerius* into two genera, *Sphaerius s.s.* (Figure 6) and *Bezesporum*, based on both morphological and molecular evidences. Extant *Bezesporum* differs from *Sphaerius s.s.* in a series of characters, including the 4-segmented antennal club, parallel-sided mentum, anteriorly converging clypeus, relatively long mesoventral plate, and metatarsus with very long setae. Typical *Sphaerius* also has a relatively narrow prosternum, whereas the prosternum of extant *Bezesporum* and a few aberrant *Sphaerius* is wider (Figure 6E). Fikáček et al. (2022) also reported the fossil *Be. burmiticum*, where the generic assignment was made based solely

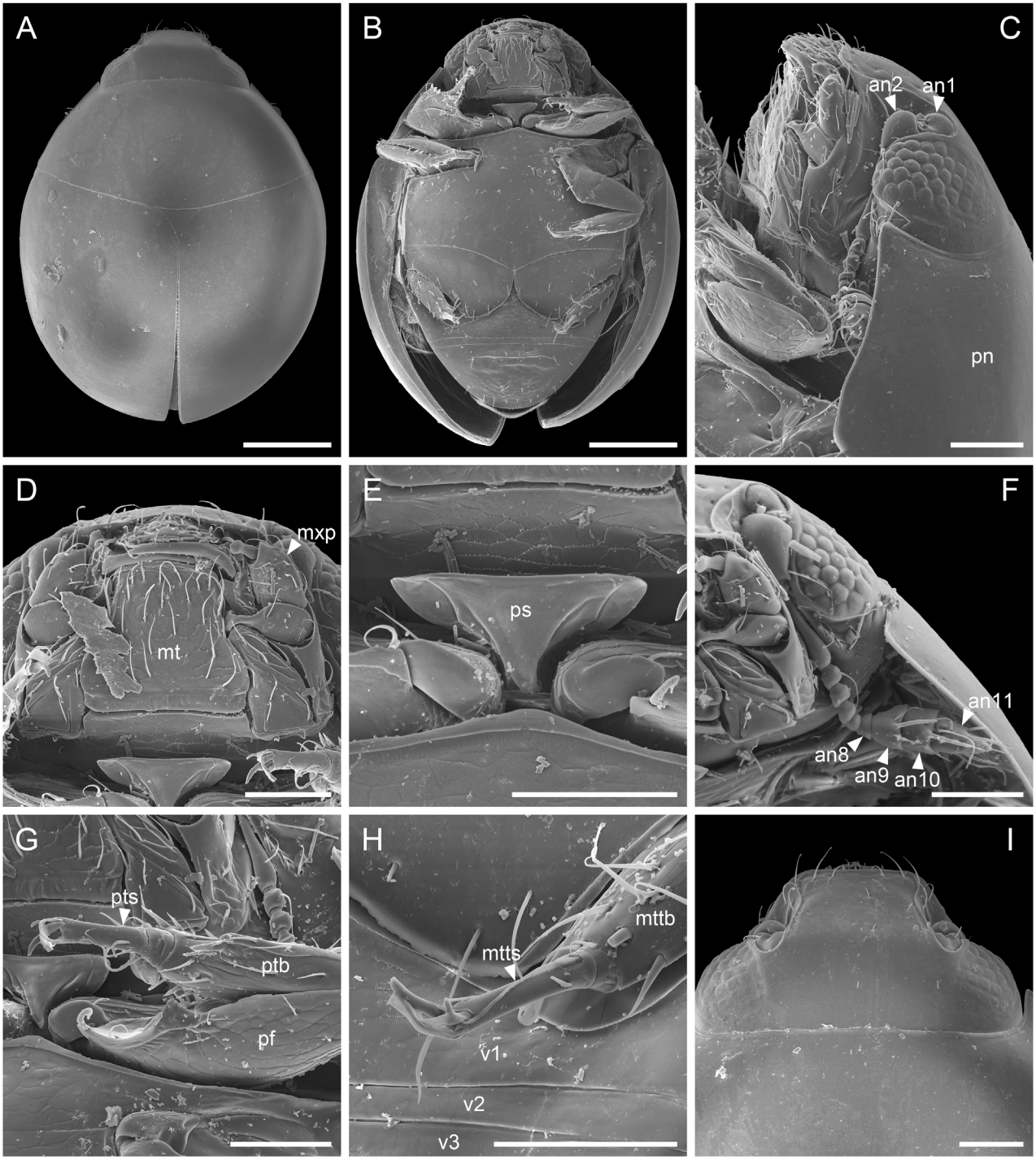

FIGURE 6
Extant *Sphaerius* sp. from Australia, under scanning electron microscopy. **(A)** Habitus, dorsal view. **(B)** Habitus, ventral view. **(C)** Head and prothorax, lateral view. **(D)** Mouthparts, ventral view. **(E)** Prosternum, ventral view. **(F)** Antenna. **(G)** Fore leg. **(H)** Metatarsus. **(I)** Head, dorsal view. Abbreviations: an1–11, antennomeres 1–11; mt, mentum; mttb, metatibia; mtts, metatarsus; mxp, maxillary palp; pf, profemur; pn, pronotum; ps, prosternum; ptb, protibia; pts, protarsus; v1–3, ventrites 1–3. Scale bars: 150 μm in **(A,B)**, 50 μm in **(C–I)**.

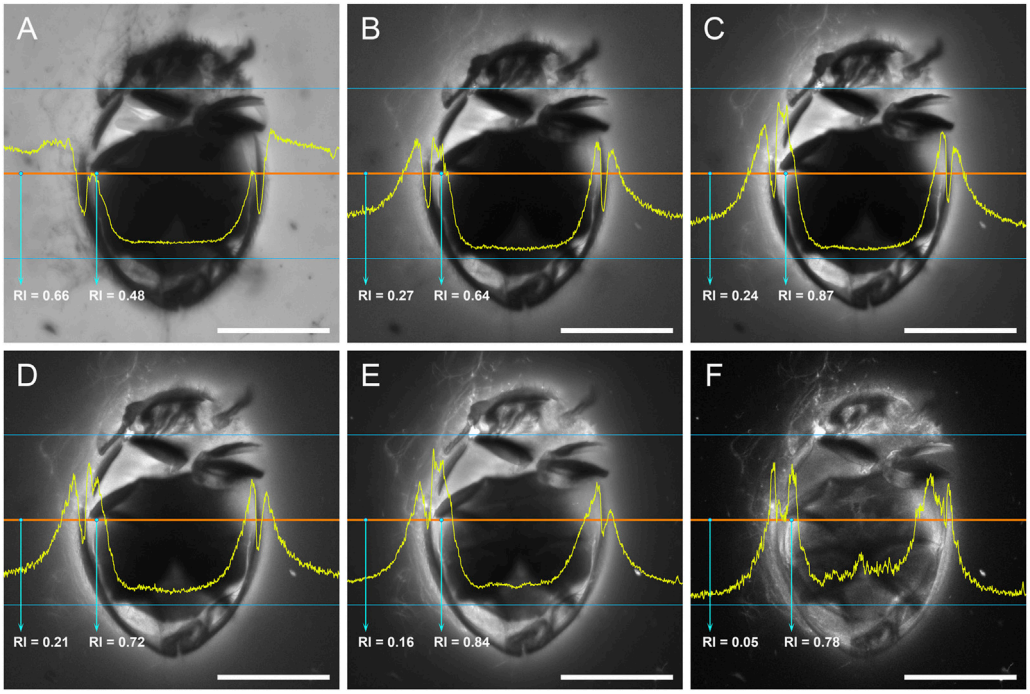

FIGURE 7
Crowsonaerius minutus in amber under confocal microscopy, excited with laser of different wavelengths. The yellow profile shows the relative intensity (RI) along the mid-section (red line). **(A)** 405 nm (Diode 450-30). **(B)** 458 nm (Argon). **(C)** 488 nm (Argon). **(D)** 514 nm (Argon). **(E)** 561 nm (DPSS 561-10). **(F)** 633 nm (HeNe633). Scale bars: 200 μm.

on the 4-segmented antennal club and the relatively long mesoventral plate. The states of other diagnostic characters mentioned above are unknown in *Be. burmiticum*.

The better preservation state and the usage of confocal microscopy enable us to extract more morphological information from the newly discovered *S. martini*. The new species generally shares more similar characters with extant *Sphaerius* (e.g., mentum, prosternum and mesoventrite). However, *S. martini* has very long setae on metatarsus and a somewhat sinuate anterior margin of mesotrochanterofemur, which are actually characteristic of *Bezesporum*, whereas such very long setae are absent and the anterior mesotrochanterofemoral margin is straight in extant *Sphaerius*. Generally *Sphaerius* should have 3-segmented antennal clubs (although some specimens from Japan or Taiwan have more or less 4-segmented antennal clubs; Kamezawa & Matsubara, 2012: figure 4A; Fikáček et al., 2022: figure 4C). The antennal club of *S. martini* is clearly 4-segmented, which has also been proposed as a diagnostic character of *Bezesporum*. As mentioned by Fikáček et al. (2022), the *Sphaerius* species from Australia and South Africa (aberrant *Sphaerius*) exhibit a somewhat intermediate morphology between *Bezesporum* and typical *Sphaerius*. The discovery of *S. martini* further highlights the morphological variability within the *Bezesporum* + *Sphaerius* group. As no molecular data are available for *S. martini* (also considering that few informative morphological characters are available for sphaeriusids), it would be hard to accurately determine its systematic position within this group. More comprehensive studies on the morphological and genetic diversity of extant Sphaeriusidae might be helpful to further justify (or reject) the separation of *Bezesporum* from *Sphaerius*.

4.2 Relationship between Sphaeriusidae and other myxophagan families

Regarding the position of Sphaeriusidae within Myxophaga, morphological phylogenetic studies have suggested a relationship of (Lepiceridae + (Torridincolidae + (Sphaeriusidae + Hydroscaphidae))) (Beutel, 1999; Lawrence et al., 2011; Yavorskaya et al., 2018; Jałoszyński et al., 2020). The monophyly of Myxophaga excluding Lepiceridae is partly supported by their distinctly reduced apical maxillary palpomere, while Lepiceridae has normal-sized apical maxillary palpomere and represents the basalmost lineage in Myxophaga. However, this morphology-based phylogeny was

not supported by molecular studies, where Sphaeriusidae was sister to Lepiceridae, and Hydroscaphidae was the basalmost lineage in Myxophaga (Mckenna et al., 2015; Mckenna et al., 2019). The discovery of unreduced apical maxillary palpomere in *Crowsonaerius* seems to be in accordance with the molecular-based phylogeny. Under this scenario, the common ancestor of Lepiceridae and Sphaeriusidae might have a normal apical maxillary palpomere, and the palpomere was later reduced in crown-group Sphaeriusidae.

4.3 Confocal imaging for fossil insects in amber

Scanning electron microscope is an excellent tool for examining the surface morphology of extant insects. SEM can achieve a higher resolution than optical methods, and therefore can properly record fine microstructures (e.g., microsculptures, hairs or sensilla). SEM is helpful for the observation of macrostructure as well. Compared with ordinary optical images, the structural boundaries are generally more clearly outlined in SEM images, especially for dark specimens (e.g., Figure 6). For the study of fossil insects in amber, fluorescence microscopy can achieve a somewhat similar purpose, where fluorescence generated around the insect surface clearly outlines the structural boundaries (Fu et al., 2021). Compared with widefield fluorescence microscopy, confocal laser scanning microscopy could further achieve a higher signal to noise ratio due to the exclusion of out of focus lights. Many studies have shown that confocal microscopy is effective for imaging insects (and other arthopods) in amber (e.g., Yamamoto et al., 2016; Li et al., 2021a; Li et al., 2021b; Su et al., 2021; Vorontsov & Voronezhskaya, 2022).

In the present study, we further test the effect of using different excitation wavelengths when imaging amber fossils with confocal microscopy. When excited with light of short wavelength (e.g., 405 nm; Figure 7A), the amber matrix has strong emission, which is consistent with previous studies (without inclusions involved) (e.g., Zhang et al., 2020a; Zhang et al., 2020b). The strong emission from the amber matrix masks the useful signal from the boundary layer between the amber matrix and the fossil inclusion; thus it is not ideal for the imaging of the inclusion. When the excitation wavelength become longer, the emission from amber matrix become weaker, and the emission from the boundary layer become comparatively stronger, which clearly illustrates the surface structures of the inclusion (Figures 7B–E). At the longest excitation wavelength we tested (633 nm; Figure 7F), the emission from amber matrix is very low, leading to the highest contrast of targeted structures. The chemical compounds behind the amber fluorescence have been suggested as various aromatic hydrocarbons (e.g., Bellani et al., 2005; Chekryzhov et al., 2014; Bechtel et al., 2016), although it is difficult to accurately determine their specific composition. It appears that during the formation of amber, the inclusion might have been involved in some chemical reactions with the amber matrix, leading to a shift of boundary layer emission toward longer wavelength (e.g., aggregation of aromatics; Vogler, 2018).

Although the exact mechanism behind this phenomenon is not yet clear, our study nevertheless suggests that using excitation light of longer wavelengths may further improve the signal to noise ratio, especially for amber specimens with strong background fluorescence. However, the emission may be too weak at the red region (e.g., when excited at 633 nm), therefore requiring a time-consuming exposure. Based on our experience, an excitation wavelength of 488–561 nm could generally produce ideal confocal photos for most inclusions from Burmese amber.

Data availability statement

The original contributions presented in the study are included in the article/Supplementary Material. The original confocal data are available in Zenodo repository (doi: 10.5281/zenodo.7319965). Further inquiries can be directed to the corresponding author.

Author contributions

C-YC and Y-DL conceived the study. C-YC, D-YH, and AS acquired and processed the specimens. Y-DL acquired and processed the photomicrographs and performed the analysis. Y-DL drafted the manuscript, to which C-YC and AS contributed. All authors commented on the manuscript and gave final approval for publication.

Funding

Financial support was provided by the Second Tibetan Plateau Scientific Expedition and Research project (2019QZKK0706), the Strategic Priority Research Program of the Chinese Academy of Sciences (XDB26000000), and the National Natural Science Foundation of China (42222201 and 42288201). Y-DL is supported by a scholarship granted by the China Scholarship Council (202108320010).

Acknowledgments

We are grateful to Martin Fikáček for the detailed discussion. We thank Rong Huang and Yan Fang for technical help with confocal imaging, and Chun-Zhao Wang for technical help with SEM imaging. The editor and two reviewers provided helpful comments on the manuscript.

Conflict of interest

The authors declare that the research was conducted in the absence of any commercial or financial relationships that could be construed as a potential conflict of interest.

Publisher's note

All claims expressed in this article are solely those of the authors and do not necessarily represent those of their affiliated organizations, or those of the publisher, the editors and the reviewers. Any product that may be evaluated in this article, or claim that may be made by its manufacturer, is not guaranteed or endorsed by the publisher.

Supplementary material

The Supplementary Material for this article can be found online at: https://www.frontiersin.org/articles/10.3389/feart.2022.901573/full#supplementary-material

References

Bechtel, A., Chekryzhov, I. Y., Nechaev, V. P., and Kononov, V. V. (2016). Hydrocarbon composition of Russian amber from the Voznovo lignite deposit and Sakhalin Island. *Int. J. Coal Geol.* 167, 176–183. doi:10.1016/j.coal.2016.10.005

Bellani, V., Giulotto, E., Linati, L., and Sacchi, D. (2005). Origin of the blue fluorescence in Dominican amber. *J. Appl. Phys.* 97, 016101. doi:10.1063/1.1829395

Beutel, R. G. (1999). Phylogenetic analysis of Myxophaga (Coleoptera) with a redescription of *Lepicerus horni* (Lepiceridae). *Zool. Anz.* 237, 291–308.

Beutel, R. G., and Raffaini, G. B. (2003). First record of Sphaeriusidae for Argentina. *Koleopterol. Rundsch.* 73, 1–6.

Cai, C., Tihelka, E., Giacomelli, M., Lawrence, J. F., Slipinski, A., Kundrata, R., et al. (2022). Integrated phylogenomics and fossil data illuminate the evolution of beetles. *R. Soc. Open Sci.* 9, 211771. doi:10.1098/rsos.211771

Chekryzhov, I. Y., Nechaev, V. P., and Kononov, V. V. (2014). Blue-fluorescing amber from Cenozoic lignite, eastern Sikhote-Alin, Far East Russia: Preliminary results. *Int. J. Coal Geol.* 132, 6–12. doi:10.1016/j.coal.2014.07.013

Fikáček, M., Beutel, R. G., Cai, C., Lawrence, J. F., Newton, A. F., Solodovnikov, A., et al. (2020). Reliable placement of beetle fossils via phylogenetic analyses – Triassic *Leehermania* as a case study (Staphylinidae or Myxophaga?) *Syst. Entomol.* 45, 175–187. doi:10.1111/syen.12386

Fikáček, M., Yamamoto, S., Matsumoto, K., Beutel, R. G., and Maddison, D. R. (2022). Phylogeny and systematics of Sphaeriusidae (Coleoptera: Myxophaga): minute living fossils with underestimated past and present-day diversity. *Syst. Entomol.* doi:10.1111/syen.12571

Fu, Y.-Z., Li, Y.-D., Su, Y.-T., Cai, C.-Y., and Huang, D.-Y. (2021). Application of confocal laser scanning microscopy to the study of amber bioinclusions. *Palaeoentomology* 4, 266–278. doi:10.11646/palaeoentomology.4.3.14

Hall, W. E. (2019). "Sphaeriusidae Erichson, 1845," in *Australian beetles. Volume 2: Archostemata, Myxophaga, adephaga, polyphaga (part).* Editors A. Ślipiski and J. F. Lawrence (Collingwood, Australia: CSIRO Publishing), 15–17.

Jałoszyński, P., Luo, X.-Z., Hammel, J. U., Yamamoto, S., and Beutel, R. G. (2020). The mid-Cretaceous †*Lepiceratus* gen. nov. and the evolution of the relict beetle family Lepiceridae (Insecta: Coleoptera: Myxophaga). *J. Syst. Palaeontol.* 18, 1127–1140. doi:10.1080/14772019.2020.1747561

Kamezawa, H., and Matsubara, Y. (2012). A faunistic note on a species of the genus *Sphaerius* Waltl, 1838 (Myxophaga, Sphaeriusidae) collected from Tamagawa river, Tokyo Metropolis, central Honshu. *Sayabane* (6), 25–27.

Kirejtshuk, A. G. (2009). A new genus and species of Sphaeriusidae (Coleoptera, Myxophaga) from Lower Cretaceous Burmese amber. *Denisia* 26, 99–102.

Lawrence, J. F., and Ślipiński, A. (2013). *Australian beetles. Volume 1: morphology, classification and keys*. Collingwood, Australia: CSIRO Publishing.

Lawrence, J. F., Ślipiński, A., Seago, A. E., Thayer, M. K., Newton, A. F., and Marvaldi, A. E. (2011). Phylogeny of the Coleoptera based on morphological characters of adults and larvae. *Ann. Zool.* 61, 1–217. doi:10.3161/000345411x576725

Letunic, I., and Bork, P. (2021). Interactive tree of life (iTOL) v5: An online tool for phylogenetic tree display and annotation. *Nucleic Acids Res.* 49, W293–W296. doi:10.1093/nar/gkab301

Li, Y.-D., Kundrata, R., Packova, G., Huang, D.-Y., and Cai, C.-Y. (2021b). An unusual elateroid lineage from mid-Cretaceous Burmese amber (Coleoptera: Elateroidea). *Sci. Rep.* 11, 21985. doi:10.1038/s41598-021-01398-w

Li, Y.-D., Newton, A. F., Huang, D.-Y., and Cai, C.-Y. (2022). The first fossil of Nossidiinae from mid-Cretaceous amber of northern Myanmar (Coleoptera: Ptiliidae). *Front. Ecol. Evol.* 10, 911512. doi:10.3389/fevo.2022.911512

Li, Y.-D., Tihelka, E., Leschen, R. A. B, Yu, Y., Ślipiński, A., Pang, H., Huang, D., et al. (2021a). An exquisitely preserved tiny bark-gnawing beetle (Coleoptera: Trogossitidae) from mid-Cretaceous Burmese amber and the phylogeny of Trogossitidae. *J. Zool. Syst. Evol. Res.* 59, 1939–1950. doi:10.1111/jzs.12515

Liang, Z.-L., and Jia, F. (2018). A new species of *Sphaerius* Waltl from China (Coleoptera, Myxophaga, Sphaeriusidae). *ZooKeys* 808, 115–121. doi:10.3897/zookeys.808.30600

Löbl, I. (1995). New species of terrestrial *Microsporus* from the Himalaya (Coleoptera: Microsporidae). *Entomol. Blätter* 91, 129–138.

Mao, Y., Liang, K., Su, Y., Li, J., Rao, X., Zhang, H., et al. (2018). Various amberground marine animals on Burmese amber with discussions on its age. *Palaeoentomology* 1, 91–103. doi:10.11646/palaeoentomology.1.1.11

McKenna, D. D., Shin, S., Ahrens, D., Balke, M., Beza-Beza, C., Clarke, D. J., et al. (2019). The evolution and genomic basis of beetle diversity. *Proc. Natl. Acad. Sci. U.S.A.* 116, 24729–24737. doi:10.1073/pnas.1909655116

McKenna, D. D., Wild, A. L., Kanda, K., Bellamy, C. L., Beutel, R. G., Caterino, M. S., et al. (2015). The beetle tree of life reveals that Coleoptera survived end-Permian mass extinction to diversify during the Cretaceous terrestrial revolution. *Syst. Entomol.* 40, 835–880. doi:10.1111/syen.12132

Mesaroš, G. (2013). Sphaeriusidae (Coleoptera, Myxophaga): A new beetle family to the fauna of Serbia. *Bull. Nat. Hist. Mus.* 6, 71–74. doi:10.5937/bnhmb1306071m

Qvarnström, M., Fikáček, M., Wernström, J. V., Huld, S., Beutel, R. G., Arriaga-Varela, E., et al. (2021). Exceptionally preserved beetles in a Triassic coprolite of putative dinosauriform origin. *Curr. Biol.* 31, 3374–3381. doi:10.1016/j.cub.2021.05.015

Reichardt, H. (1973). A critical study of the suborder Myxophaga, with a taxonomic revision of the Brazilian Torridincolidae and Hydroscaphidae (Coleoptera). *Arq. Zool.* 24, 73–162. doi:10.11606/issn.2176-7793.v24i2p73-162

Ronquist, F., Teslenko, M., Van Der Mark, P., Ayres, D. L., Darling, A., Höhna, S., et al. (2012). MrBayes 3.2: Efficient Bayesian phylogenetic inference and model choice across a large model space. *Syst. Biol.* 61, 539–542. doi:10.1093/sysbio/sys029

Shi, G., Grimaldi, D. A., Harlow, G. E., Wang, J., Wang, J., Yang, M., et al. (2012). Age constraint on Burmese amber based on U-Pb dating of zircons. *Cretac. Res.* 37, 155–163. doi:10.1016/j.cretres.2012.03.014

Su, Y.-T., Cai, C.-Y., and Huang, D.-Y. (2021). Morphological revision of *Siphonophora hui* (Myriapoda: Diplopoda: Siphonophoridae) from the mid-

Cretaceous Burmese amber. *Palaeoentomology* 4, 279–288. doi:10.11646/palaeoentomology.4.3.15

Vogler, A. (2018). Photoluminescence of Baltic amber. *Z. Naturforsch. B* 73, 673–675. doi:10.1515/znb-2018-0106

Vorontsov, D., and Voronezhskaya, E. E. (2022). Pushing the limits of optical resolution in the study of the tiniest fossil arthropods. *Hist. Biol.* 34, 2415–2423. doi:10.1080/08912963.2021.2017920

Yamamoto, S., Maruyama, M., and Parker, J. (2016). Evidence for social parasitism of early insect societies by Cretaceous rove beetles. *Nat. Commun.* 7, 13658. doi:10.1038/ncomms13658

Yavorskaya, M. I., Anton, E., Jałoszyński, P., Polilov, A., and Beutel, R. G. (2018). Cephalic anatomy of Sphaeriusidae and a morphology-based phylogeny of the suborder Myxophaga (Coleoptera). *Syst. Entomol.* 43, 777–797. doi:10.1111/syen.12304

Zhang, Z., Jiang, X., Wang, Y., Kong, F., and Shen, A. H. (2020b). Fluorescence characteristics of blue amber from the Dominican Republic, Mexico, and Myanmar. *Gems Gemol.* 56, 484–496. doi:10.5741/gems.56.4.484

Zhang, Z., Jiang, X., Wang, Y., Shen, A. H., and Kong, F. (2020a). Fluorescence spectral characteristic of amber from Baltic Sea region, Dominican republic, Mexico, Myanmar and China. *J. Gems Gemol.* 22, 1–11.